Inorg. Chem. **2004**, *43*, 5725–5735

Steric and Hydrogen-Bonding Effects on the Stability of Copper Complexes with Small Molecules

Akira Wada,[†] Yasutaka Honda,[†] Syuhei Yamaguchi,[†] Shigenori Nagatomo,[‡] Teizo Kitagawa,[‡] Koichiro Jitsukawa,[†] and Hideki Masuda*,[†]

Department of Applied Chemistry, Nagoya Institute of Technology, Gokiso-cho, Showa-ku, Nagoya 466-8555, Japan, and Center of Integrative Bioscience, Okazaki National Research Institutes, Myodaiji, Okazaki 444-8585, Japan

Received March 15, 2004

A series of the copper(II) complexes with tripodal tetradentate tris(pyridyl 2-methyl)amine-based ligands possessing the hydrogen-bonding 6-aminopyridine units (tapa, three amino groups; bapa, two amino groups; mapa, one amino group) have been synthesized, and their copper(II) complexes with a small molecule such as dioxygen and azide have been studied spectroscopically and structurally. The reaction of their Cu(II) complexes with NaN_3 have given the mononuclear copper complexes with azide in an end-on mode, $[Cu(tapa)(N_3)]ClO_4$ (**1a**), $[Cu(bapa)(N_3)]ClO_4$ (**2a**), $[Cu(mapa)(N_3)]ClO_4$ (**3a**), and $[Cu(tpa)(N_3)]ClO_4$ (**4a**) (tpa, no amino group). The crystal structures have revealed that the coordination geometries around the metal centers are almost a trigonal-bipyramidal rather than a square-planar except for **1a** with an intermediate between them. The UV–vis and ESR spectral data indicate that the increase of NH_2 groups of ligands causes the structural change from trigonal-bipyramidal to square-pyramidal geometry, which is regulated by a combination of steric repulsion and hydrogen bond. The steric repulsion of amino groups with the azide nitrogen gives rise to elongation of the $Cu–N_{py}$ bonds, which leads to the positive shift of the redox potentials of the complexes. The hydrogen bonds between the coordinated azide and amino nitrogens (2.84–3.05 Å) contribute clearly to the fixation of azide. The Cu(I) complexes with bapa and mapa ligands have been obtained as a precipitate, although that with tapa was not isolated. The reactions of the Cu(I) complexes with dioxygen in MeOH at −75 °C have given the trans-μ-1,2 peroxo dinuclear Cu(II) complexes formulated as $[\{(tapa)Cu\}_2(O_2)]^{2+}$ (**1c**), $[\{(bapa)Cu\}_2(O_2)]^{2+}$ (**2c**), and $[\{(mapa)Cu\}_2(O_2)]^{2+}$ (**3c**), whose characterizations were confirmed by UV–vis, ESR, and resonance Raman spectroscopies. UV–vis spectra of **1c**, **2c**, and **3c** exhibited intense bands assignable to $\pi^*(O_2^{2-})$-to-d(Cu) charge transfer (CT) transitions at λ_{max}/nm (ϵ/$M^{-1}cm^{-1}$) = 449 (4620), 474 (6860), and 500 (9680), respectively. The series of the peroxo adducts generated was ESR silent. The resonance Raman spectra exhibited the enhanced features assignable to two stretching vibrations $\nu(^{16}O–^{16}O/^{18}O–^{18}O)/cm^{-1}$ and $\nu(Cu–^{16}O/Cu–^{18}O)/cm^{-1}$ at 853/807 (**1c**), 858/812 (**2c**), 847/800 (**3c**), and at 547/522 (**2c**), 544/518 (**3c**), respectively. The thermal stability of the peroxo-copper species has increased with increase in the number of the hydrogen-bonding interactions between the peroxide and amino groups.

Introduction

A large number of proteins utilizing mono-/di-copper ions as active sites perform diverse functions such as reversible dioxygen binding and oxygen activations in biological systems.[1–3] Recently, in elucidation for the specific role of the active sites and physicochemical properties of copper−oxygen intermediates proposed in these biological reactions, the chemical approach based on the construction of their structural/functional models[4–10] has been the focus of

* Author to whom correspondence should be addressed.Tel: +81-52-735-5228. Fax: +81-52-735-5209. E-mail: masuda.hideki@nitech.ac.jp.
[†] Nagoya Institute of Technology.
[‡] Okazaki National Research Institutes.

(1) Solomon, E. I.; Sundaram, U. M.; Machonkin, T. E. *Chem. Rev.* **1996**, *94*, 2563.
(2) Klinman, J. P. *Chem. Rev.* **1996**, *96*, 2541.
(3) Kaim, W.; Rall, J. *Angew. Chem., Int. Ed. Engl.* **1996**, *35*, 43.
(4) Solomon, E. I.; F. Tuczek, F.; Root, D. E.; Brown, C. A. *Chem. Rev.* **1994**, *94*, 827.
(5) Kitajima, N.; Moro-oka, Y. *Chem. Rev.* **1994**, *94*, 737.
(6) Fontecave, M.; Pierre, J.-L. *Coord. Chem. Rev.* **1998**, *170*, 125.

10.1021/ic0496572 CCC: $27.50
Published on Web 08/04/2004

Chart 1. Tripodal Pyridylamine Ligands (L)

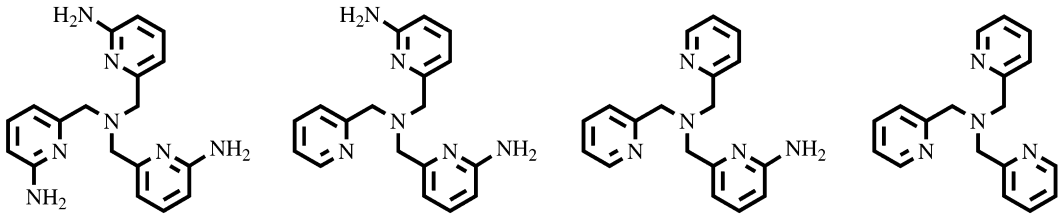

TAPA BAPA MAPA TPA

TAPA : tris(6-amino-2-pyridylmethyl)amine
BAPA : bis(6-amino-2-pyridylmethyl)(2-pyridylmethyl)amine
MAPA : mono(6-amino-2-pyridylmethyl)bis(2-pyridylmethyl)amine
TPA : tris(2-pyridylmethyl)amine

considerable interest. Thus, the related efforts have emphasized the reactivity of synthetic Cu(I) complexes with dioxygen and characterization of the peroxo-copper adducts. Karlin[11−13] and Kitajima[14,15] reported first the structurally characterized peroxo dinuclear Cu(II) complexes as models for dioxygen binding in oxy-hemocyanin (oxy-Hc).[4,5] For example, the spectroscopic studies on oxygenation of the Cu(I) complex with tripodal ligand, tris(2-pyridylmethyl)-amine (tpa), revealed the formation of the peroxo dinuclear Cu(II) complex formulated as $[\{(tpa)Cu\}_2(O_2)]^{2+}$, and the X-ray crystal structure established that the peroxide anion is bridged between two Cu(II) sites in a trans-μ-1,2 mode.[11,12] There are also some recent reports on the preparations and characterizations of trans-μ-1,2-peroxo dinuclear Cu(II) complexes.[16−21] On the other hand, the studies of μ-η^2:η^2 (side-on) peroxo dinuclear Cu(II) complex $\{Cu[HB(3,5\text{-}^iPr_2pz)_3]\}_2(O_2)$ utilizing sterically demanding ligand, tris(3,5-diisopropylpyrazolyl)borate ($HB(3,5\text{-}^iPr_2pz)_3$), demonstrated that the peroxide binding of oxy-Hc results in the formation of side-on peroxo-dicopper unit at active site.[5,14,15] These structural and spectroscopic characterizations of the peroxo Cu(II) dimers have provided remarkable advances in copper/dioxygen chemistry and inorganic biochemistry.[1−10]

At this stage, it is very important to perform electronic and geometric studies of the copper−oxygen interactions in biological systems by the use of model copper complexes with appropriately modified ligands. From such a viewpoint, we previously studied the thermal stability and spectroscopic behavior of μ-peroxo dicopper(II) complexes with intramolecular hydrogen bonding site and/or steric group to examine the effect of the proximal hydrogen bonding and steric interactions in μ-peroxo dicopper(II) complexes using the ligands mono(6-amino-2-pyridylmethyl)bis(2-pyridylmethyl)amine (mapa), mono(6-pivalamido-2-pyridylmethyl)-bis(2-pyridylmethyl)amine (mppa), bis(2-pyridylmethyl)(6-methyl-2-pyridylmethyl)amine (6-Metpa), and tpa.[22] Here, to clarify the effect of further hydrogen bonding interaction, the mononuclear Cu(II) complexes with azide, $[Cu(L)(N_3)]^+$, and trans-μ-1,2 peroxo Cu(II) dimers, $[\{(L)Cu\}_2(O_2)]^{2+}$, were prepared using some tripodal pyridylamine ligands L, as shown in Chart 1 and their structural/spectroscopic characterizations were carried out. Especially, we will discuss in detail the effect of hydrogen bonding and steric interactions of amino substitutions for the electronic property and stability of $[\{(L)Cu\}_2(O_2)]^{2+}$ which have been determined by structural, electrochemical, and spectroscopic analysis.

Experimental Section

Synthesis of Tripodal Pyridylamine Ligands. The tripodal ligands, tpa[12] and mapa,[22] were prepared by the method previously reported. The other ligands with NH_2 amino groups on pyridine 6-positions of tpa, tapa, and bapa, were synthesized according to the procedures below. Their formulation and purity were confirmed by ^{1}H NMR and FT-IR spectroscopies and elemental analysis.

Synthesis of Tris(6-amino-2-pyridylmethyl)amine (tapa). To an EtOH solution (500 mL) containing tris(6-pivalamido-2-pyridylmethyl)amine (TPPA) (5.88 g, 0.01 mol) previously reported[23] was added a small amount of H_2O containing KOH (28.1 g, 0.50 mol), and then stirred at 60 °C for a few days. After the solution was cooled and solvents were removed under vacuum, the resulting residue was dissolved in MeOH−H_2O solution (MeOH/H_2O = 1:15, 300 mL) to give white precipitate, which was washed by an excess

(7) Mirica, L. M.; Ottenwaelder, X.; Stack, T. D. P. *Chem. Rev.* **2004**, *104*, 1013.
(8) Lewis, E. A.; Tolman, W. B. *Chem. Rev.* **2004**, *104*, 1047.
(9) Blackman, A. G.; Tolman, W. B. In *Structure and Bonding*; Meunier, B., Ed.; Springer-Verlag: Berlin, 2000; Vol. 97, p 179.
(10) Schindler, S. *Eur. J. Inorg. Chem.* **2000**, 2311.
(11) Jacobson, R. R.; Tyeklár, Z.; Farooq, A.; Kralin, K. D.; Liu, S.; Zubieta, J. *J. Am. Chem. Soc.* **1988**, *110*, 3690.
(12) Tyeklár, Z.; Jacobson, R. R.; Wei, N.; Murthy, N. N.; Zubieta, J.; Karlin, K. D. *J. Am. Chem. Soc.* **1993**, *115*, 2677.
(13) Karlin, K. D.; Kaderli, S.; Zuberbühler, A. D. *Acc. Chem. Res.* **1997**, *30*, 139 and references therein.
(14) Kitajima, N.; Fujisawa, K.; Moro-oka, Y.; Toriumi, K. *J. Am. Chem. Soc.* **1989**, *111*, 8975.
(15) Kitajima, N.; Fujisawa, K.; Fujimoto, C.; Moro-oka, Y.; Hashimoto, S.; Kitagawa, T.; Toriumi, K.; Tatsumi, K.; Nakamura, A. *J. Am. Chem. Soc.* **1992**, *114*, 1277.
(16) Schatz, M.; Becker, M.; Thaler, F.; Hampel, F.; Schindler, S.; Jacobson, R. R.; Tyeklár, Z.; Murthy, N. N.; Ghosh, P.; Chen, Q.; Zubieta, J.; Karlin, K. D. *Inorg. Chem.* **2001**, *40*, 2312.
(17) Zhang, C. X.; Kaderli, S.; Costas, M.; Kim, E.; Neuhold, Y.-M.; Karlin, K. D.; Zuberbühler, A. D. *Inorg. Chem.* **2003**, *42*, 1807.
(18) Becker, M.; Heinemann, F. W.; Schindler, S. *Chem. Eur. J.* **1999**, *5*, 3124.
(19) Weitzer, M.; Schindler, S.; Brehm, G.; Schneider, S.; Hörmann, E.; Jung, B.; Kaderli, S.; Zuberbüler, A. D. *Inorg. Chem.* **2003**, *42*, 1800.
(20) Schatz, M.; Becker, M.; Walter, O.; Liehr, G.; Schindler, S. *Inorg. Chim. Acta* **2001**, *324*, 173.
(21) Komiyama, K.; Furutachi, H.; Nagatomo, S.; Hashimoto, A.; Hayashi, H.; Fujinami, S.; Suzuki, S.; Kitagawa, T. *Bull. Chem. Soc. Jpn.* **2004**, *77*, 59.
(22) Yamaguchi, S.; Wada, A.; Funahashi, Y.; Nagatomo, S.; Kitagawa, T.; Jitsukawa, K.; Masuda, H. *Eur. J. Inorg. Chem.* **2003**, 4378.
(23) Harata, M.; Jitsukawa, K.; Masuda, H.; Einaga, H. *Chem. Lett.* **1995**, 61.

amount of H_2O. After the usual workup, the pale yellow powder of tapa was isolated through the recrystallization from MeOH−H_2O solution; yield 2.35 g (70%). ^{1}H NMR (δ/ppm from TMS in DMSO-d_6) δ = 3.48 (s, 6H, −CH_2−), 5.76 (s, 6H, amine-N*H*), 6.28 (d, J = 8.1 Hz, 3H, py-H_5), 6.74 (d, J = 7.5 Hz, 3H, py-H_3), 7.33 (t, J = 7.5 Hz, 3H, py-H_4). Calcd for $C_{18.5}H_{23}N_7O_{0.5}$: C, 63.23; H, 6.60; N, 27.90. Found: C, 63.50; H, 6.37; N, 27.90.

Synthesis of Bis(6-amino-2-pyridylmethyl)(2-pyridylmethyl)-amine (bapa). According to the same procedure as that of tapa, the ligand bapa was synthesized by hydrolysis of bis(6-pivalamido-2-pyridylmethyl)(2-pyridylmethyl)amine (BPPA) (4.88 g, 0.01 mol) described in the literature.[24] The pale yellow powder of bapa was obtained by the recrystallization from $CHCl_3$−MeOH mixture; Yield 1.60 g (50%). ^{1}H NMR (δ/ppm from TMS in DMSO-d_6) δ = 3.50 (s, 4H, −CH_2−), 3.73 (s, 2H, −CH_2−), 5.81 (s, 4H, amine-N*H*), 6.29 (d, J = 7.8 Hz, 2H, py-H_5), 6.75 (d, J = 7.2 Hz, 2H, py-H_3), 7.24 (t, J = 6.1 Hz, 1H, py-H_4), 7.35 (t, J = 7.5 Hz, 2H, py-H_4), 7.62 (d, J = 7.2 Hz, 1H, py-H_3), 7.77 (t, J = 7.5 Hz, 1H, py-H_5), 8.48 (d, J = 6.0 Hz, 1H, py-H_6). Calcd for $C_{18}H_{21}N_6O_{0.5}$: C, 65.63; H, 6.43; N, 25.51. Found: C, 65.68; H, 6.15; N, 25.81.

Preparation of Copper Complexes, [Cu(tapa)(N_3)]ClO_4 (1a), [Cu(bapa)(N_3)]ClO_4 (2a), [Cu(mapa)(N_3)]ClO_4 (3a), and [Cu(tpa)-(N_3)]ClO_4 (4a). The preparation of **3a**[22] and **4a**[22,25] were performed by previously reported methods. The other copper(II)-azide complexes, **1a** and **2a,** were synthesized by the below procedures. The formulation and purity of all mononuclear Cu(II) complexes with azide prepared by the following methods were identified by elemental analysis and ESI mass spectroscopy. All the complexes were characterized by X-ray crystallography.

The following copper ions, $[Cu^I(MeCN)_4]ClO_4$, $[Cu^I(MeCN)_4]$-PF_6, and $Cu^{II}(ClO_4)_2\cdot 6H_2O$, were used as the starting materials of Cu(I) and Cu(II) ions, respectively. *Caution: The perchlorate salts are potentially explosive and should be handled with care.*

[Cu(tapa)(N_3)]ClO_4 (1a). To a stirred MeOH solution (7.0 mL) containing $Cu(ClO_4)_2\cdot 6H_2O$ (0.22 g, 0.60 mmol) and tapa (0.20 g, 0.60 mmol) was added NaN_3 (0.04 g, 0.62 mmol). After removing solvent in vacuo until the total volume was smaller than one-third, the green precipitate was obtained. The crystallization from the MeCN−Et_2O solution produced the crystals of [Cu(tapa)(N_3)]ClO_4 suitable for ESI mass spectroscopy, elemental, and X-ray structure analysis. Calcd for $C_{18}H_{21}N_{10}O_4ClCu$: C, 40.00; H, 3.91; N, 25.91. Found: C, 40.03; H, 3.84; N, 25.63. MS (ESI, m/z) 440 $[Cu(tapa)]^+$.

[Cu(bapa)(N_3)]ClO_4 (2a). The preparation of [Cu(bapa)(N_3)]-ClO_4 (**2a**) was performed by the same method as **1a**. **2a**$\cdot 0.5H_2O$, Calcd for $C_{18}H_{21}N_9O_{4.5}ClCu$: C, 40.45; H, 3.96; N, 23.58. Found: C, 40.37; H, 3.63; N, 23.43. MS (ESI, m/z) 425 $[Cu(bapa)(N_3)]^+$.

Preparation of Copper(I) Complexes of [Cu(bapa)]PF_6 (2b) and [Cu(mapa)]PF_6 (3b). To prepare the μ-peroxo dicopper(II) complexes, we synthesized [Cu(bapa)]PF_6 (**2b**) and [Cu(mapa)]-PF_6 (**3b**) as starting materials. The ligands bapa (8.0 mg, 25 μmol) or mapa (7.6 mg, 25 μmol) were dissolved in 3 mL of EtOH/MeCN and added dropwise to 9.3 mg (25 μmol) of $[Cu(MeCN)_4]PF_6$ under anaerobic conditions (high concentration of Cu(I) salts in alcohol solvent tends to undergo disproportionation of them to a Cu(II) salt and copper metal). Then, the resulting solutions were layered with diethyl ether. After standing for a few days, the crystals of the corresponding Cu(I) complexes suitable for elemental analysis were obtained.

[Cu(bapa)]PF_6, Calcd for $C_{18}H_{20}N_6F_6PCu$: C, 40.88; H, 3.81; N, 15.88. Found: C, 41.17; H, 3.94; N, 16.06.

[Cu(mapa)]$PF_6\cdot 1/4EtOH\cdot 1/4MeCN$, Calcd for $C_{19}H_{21.25}N_{5.25}O_{0.25}F_6$-PCu: C, 42.60; H, 4.00; N, 13.73. Found: C, 42.55; H, 3.89; N, 13.68.

Generation of Peroxo Dicopper Complexes, [{(tapa)Cu}$_2$-(O_2)]$^{2+}$ (1c), [{(bapa)Cu}$_2$(O_2)]$^{2+}$ (2c), and [{(mapa)Cu}$_2$(O_2)]$^{2+}$ (3c). Generation of μ-peroxo-dicopper(II) complexes was performed as follows. [Cu(bapa)]PF_6 (**2b**) or [Cu(mapa)]PF_6 (**3b**) was dissolved into deaerated MeOH or EtOH under anaerobic conditions and then the resultant solutions were cooled to −75 °C. In the case of the use of ligand tapa, the corresponding Cu(I) complex was prepared by mixing equimolar amounts of the tapa ligand and $[Cu(MeCN)_4]X$ (X = PF_6 or ClO_4)), which was cooled to the same temperature. After the introduction of O_2 gas into the solutions by gentle bubbling, the color changed from yellow to brown or purple due to the formation of the μ-peroxo dicopper complexes [{(tapa)-Cu}$_2$(O_2)]$^{2+}$ (**1c**) (yellow to brown), [{(bapa)Cu}$_2$(O_2)]$^{2+}$ (**2c**) (yellow to brown purple), and [{(mapa)Cu}$_2$(O_2)]$^{2+}$ (**3c**) (yellow to red purple) were observed. The formulation and spectroscopic characterization of these complexes were identified by UV−vis, ESR, ESI mass, and resonance Raman spectroscopic measurements.

Kinetic experiments were carried out under the following conditions. The decay rates of **1c**, **2c**, and **3c** were measured at −50 °C in MeOH by monitoring a decrease of the characteristic CT bands at 449, 474, and 500 nm, respectively. The decomposition of all peroxo Cu(II) complexes obeyed first-order kinetics. The first-order rate constant k_{dec} for the decay of the μ-peroxo dicopper complexes was calculated by least-squares treatment of data using the following equation:

$$\ln\{([A_t] - [A_f])/([A_0] - [A_f])\} = -k_{dec}t$$

where A_f and A_0 are the final and initial absorbance, respectively, and A_t is the absorbance at time t.

Physical Measurements. UV−vis absorption spectra were taken using a JASCO UVIDEC-660 spectrophotometer with a thermostated cell holder designed for low-temperature experiments. X-band ESR spectra of frozen solutions were recorded at 77 K by using a JEOL RE-1X ESR spectrometer. ^{1}H NMR spectra in $CDCl_3$ and DMSO-d_6 with TMS as an internal standard were performed on a Gemini 300 MHz NMR spectrometer. IR spectra were measured as KBr pellets and acetonitrile solutions using a Jasco FT/IR-410 spectrometer.

All mass spectra were acquired using an API 300 triple quadrupole mass spectrometer equipped with an ionspray interface (PE-Sciex, Thornhill, ON). Instrument settings, data acquisition, and data processing were controlled by a Macintosh 8500/150 computer. Samples were introduced using a dual syringe pump (Harvard Apparatus, South Natick, MA) fitted with Hamilton syringes (Hamilton Co, Reno, NV). The samples for all spectral measurements, as described above, were prepared in MeCN or MeOH.

Electrochemical measurements were performed with a BAS CV-50W voltammetric analyzer. Cyclic voltammograms were obtained by using a three- component system consisting of a glassy carbon working electrode, a platinum wire auxiliary electrode, and a saturated calomel reference electrode. All measurements were made under Ar atmosphere in MeOH solution with 0.1 M tetrabutylammonium tetrafluoroborate as the supporting electrolyte. The electrochemical potentials were corrected by measurement of ferrocene/ ferricenium couple.

Resonance Raman spectra were detected with a liquid-nitrogen-cooled CCD detector (model LN/CCD-1300-PB, Princeton Instrument) attached to a 100-cm single polychromator (model MC-

(24) Harata, M.; Hasegawa, K.; Jitsukawa, K.; Masuda, H.; Einaga, H. *Bull. Chem. Soc. Jpn.* **1998**, *71*, 1031.
(25) Lee, D. H.; Murthy, N. N.; Karlin, K. D. *Inorg. Chem.* **1997**, *36*, 5785.

Table 1. Crystallographic Data for **1a**, **2a**, **3a**, and **4a**

	1a	2a	3a	4a
formula	$C_{18}H_{21}ClCuN_{10}O_4$	$C_{18}H_{20}ClCuN_9O_4$	$C_{36}H_{38}Cl_2Cu_2N_{16}O_8$	$C_{18}H_{18}ClCuN_7O_4$
fw	540.43	525.41	1020.80	495.38
color, cryst habit	green, block	green, block	green, block	green, plate
cryst syst	monoclinic	monoclinic	triclinic	monoclinic
space group	$P2_1/n$ (No. 14)	$P2_1/n$ (No. 14)	$P\bar{1}$ (No. 2)	$P2_1/c$ (No. 14)
a/Å	11.104(2)	13.175(2)	12.765(9)	15.22(1)
b/Å	14.500(1)	14.053(3)	16.814(3)	9.038(7)
c/Å	14.272(1)	13.558(2)	12.582(4)	14.94(1)
α/deg			102.22(2)	
β/deg	100.152(10)	115.107(1)	111.58(2)	94.668(9)
γ/deg			110.20(3)	
V/Å^3	2261.9(4)	2273.1(6)	2172(2)	2148(2)
Z	4	4	2	4
D_{calcd}/g cm^{-3}	1.587	1.535	1.607	1.606
F (000)	1108.00	1076.00	1044.00	1012.00
μ/cm^{-1}	28.81 (Cu Kα)	11.23 (Mo Kα)	11.72 (Mo Kα)	12.39 (Mo Kα)
λ / Å	1.54178	0.71069	0.71070	0.71070
T/K	298	298	298	173
no. of reflns measured	3535	3859	6341	7006
no. of reflns used ($I > 2\sigma(I_0)$)	2049	1425	4333	1498
R_1[a]/R_w[b]	0.068/0.097	0.057/0.065	0.077/0.125	0.060/0.127
GOF	1.323	1.107	1.297	1.163

[a] $R_1 = \sum||F_o| - |F_c||/\sum|F_o|$. [b] $R_w = [\sum w(F_o^2 - F_c^2)^2/\sum w(F_o^2)^2]^{1/2}$.

100DG, Ritsu Oyo Kogaku). The excitation was provided by the 476.5 nm line of an Ar laser (model GLG3200, NEC). The $^{16}O_2$ samples were prepared via bubbling of dry dioxygen into MeOH solutions of the Cu(I) complexes with amino-substituted ligands at −75 °C. Isotopic substitution of the peroxo oxygens bridging the dicopper ions (**1c**, **2c**, and **3c**) was accomplished by oxygenation of the Cu(I) complexes with $^{18}O_2$. All measurements were carried out with spinning cell kept at −75 °C by a stream of liquid N_2 gas.

X-ray Crystallography of 1a, 2a, 3a, and 4a. Single crystals of **1a**, **2a**, **3a**, and **4a** suitable for X-ray diffraction measurements were obtained from the corresponding solutions by allowing the solutions to stand a few days at room temperature. The crystals were mounted on a glass capillary, and the diffraction data were collected on various X-ray instruments as described below. Crystallographic and diffraction data were obtained as below: **1a**, Rigaku AFC-5R four-circle diffractometer with graphite monochromated Cu Kα radiation at room temperature; **2a**, Enraf-Nonius CAD4-EXPRESS four-circle diffractometer with graphite monochromated Mo Kα radiation at room temperature; **3a**, a Rigaku RAXIS-IV imaging plate area detector using graphite monochromated Mo Kα radiation at room temperature; **4a**, Rigaku/MSC Mercury CCD using graphite monochromated Mo Kα radiation at −100 °C. The crystallographic data and experimental details are listed in Table 1.

The structures of **1a**, **2a**, **3a**, and **4a** were solved by a combination of direct methods and expanded using the Fourier technique.[26] Atomic scattering factors and anomalous dispersion terms were taken from International Tables for X-ray Crystallography IV.[27] All non-hydrogen atoms were refined by a full-matrix least-squares method with anisotropic displacement parameter. All the positions of hydrogen atoms were determined from difference Fourier maps, but they were not included for the refinements. All calculations were performed using the *teXsan* crystallographic software package of Molecular Structure Corporation.[28]

Results and Discussion

Preparation of Mononuclear Copper(II) Complexes with Azide. Preparation of mononuclear Cu(II) complexes with azide ion $[Cu(tapa)(N_3)]^+$ (**1a**), $[Cu(bapa)(N_3)]^+$ (**2a**), $[Cu(mapa)(N_3)]^+$ (**3a**), and $[Cu(tpa)(N_3)]^+$ (**4a**) was carried out by reaction of the appropriate tripodal ligands with equimolar amounts of $Cu(ClO_4)_2\cdot 6H_2O$ and NaN_3 in MeOH. The dark green crystals of **1a**, **2a**, **3a**, and **4a** were obtained by vapor diffusion of Et_2O into the corresponding reaction solutions. The formulations of $[Cu(L)(N_3)]^+$ were confirmed by elemental analysis. The ESI mass spectral measurements for MeOH solutions containing **1a**, **2a**, **3a**, and **4a** at room temperature showed positive ion spectra with prominent peaks at m/z 440, 425, 410, and 395, respectively. The distribution of isotopomers agreed well with calculated isotopic patterns for $[Cu(L)(N_3)]^+$, suggesting that the mononuclear Cu(II) complexes with an azide ion are stable in the solutions.

UV−vis and ESR Spectroscopies of 1a, 2a, 3a, and 4a. As depicted in Figure 1, the UV−vis spectra of **1a**, **2a**, **3a**, and **4a** in MeOH exhibited two well-separated d−d bands at ∼670 and ∼880 nm and intense ones at 385 (ϵ = 1960 M^{-1}cm^{-1}), 393 (ϵ = 2630 M^{-1}cm^{-1}), 403 (ϵ = 2940 M^{-1}cm^{-1}), and 413 nm (ϵ = 3470 M^{-1}cm^{-1}), respectively, which are assignable to the ligand-to-metal charge transfer (LMCT) transition from azide to Cu(II) ion.[29] It is noted that the LMCT bands shifted toward shorter wavelength region in the order of **1a** < **2a** < **3a** < **4a** with decrease in the absorption intensities. Interestingly, the order is well consistent with increase in the number of NH_2 substituent groups introduced at the pyridine 6-position of ligands. These are summarized in Table 2. The spectral behaviors of **2a**, **3a**,

(26) Beurskens, P. T.; Admiraal, G.; Beurskens, G.; Bosman, W. P.; DeGelder, R.; Israel, R.; Smits, J. M. M. *The DIRDIF-94 program system, Technical Report of the Crystallography Laboratory*; University of Nijmegen: The Netherlands, 1994.
(27) Ibers, J. A., Hamilton, W. C., Eds. *International Tables for X-ray Crystallography*, Vol. IV; Kynoch Press: Birmingham, UK, 1974.
(28) *teXsan, Crystal Structure Analysis Package*; Molecular Structure Corporation, 1992.
(29) Karlin, K. D.; Cohen, B. I.; Hayes, J. C.; Farooq, A.; Zubieta, J. *Inorg. Chem.* **1987**, *26*, 147 and references therein.

Table 2. Spectral Data and Electrochemical Data for $[Cu(L)(N_3)]^+$ Complexes (**1a**, **2a**, **3a**, and **4a**) in MeOH

	UV−vis spectral data		ESR spectral data				electrochemical data[a]			
ligand (L)	LMCT[b]/nm (ϵ/$M^{-1}cm^{-1}$)	d−d/nm (ϵ/$M^{-1}cm^{-1}$)	$g_{\|\|}$	$g_\perp$	$\|A_{\|\|}\|$/G	$\|A_\perp\|$/G	E_{pa}/V	E_{pc}/V	ΔE/V	$E_{1/2}$/V
tapa (**1a**)	385 (1960)	676 (310), 870 (230)	2.27	2.08	153		−0.30	−0.21	0.09	−0.27
bapa (**2a**)	393 (2630)	673 (240), 885 (230)	2.01	2.23	70	104	−0.38	−0.29	0.09	−0.33
mapa (**3a**)	403 (2940)	673 (280), 884 (270)	2.00	2.21	76	100	−0.42	−0.33	0.09	−0.37
tpa (**4a**)	413 (3470)	672 (350), 879 (310)	2.00	2.19	82	92	−0.40	−0.31	0.09	−0.36

[a] Reduction and oxidation potentials are given vs SCE. [b] LMCT (N_3^- → Cu(II)).

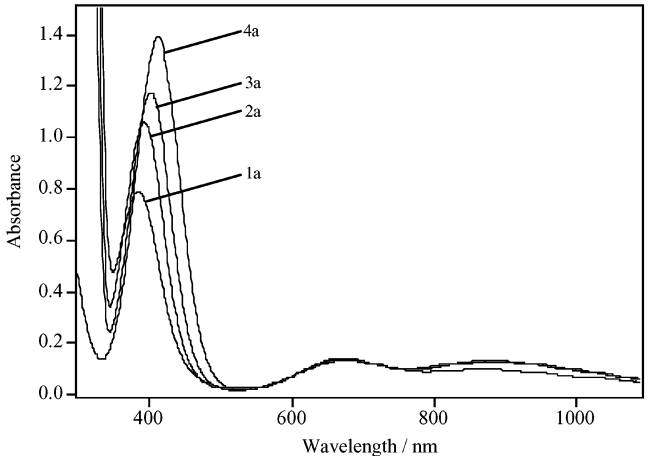

Figure 1. UV-vis spectra of $[Cu(L)(N_3)]^+$ (**1a**, **2a**, **3a**, and **4a**) in MeOH at 20 °C.

and **4a** in the d−d region (but no for that of **1a**) are characteristic for a mononuclear Cu(II) complex with a trigonal bipyramidal (TBP) geometry.[30,31] The absorption band near 870 nm in **1a** was weak in comparison with those of the other azide complexes, indicating that the Cu(II) center coordinated by tapa ligand prefers a square pyramidal (SP) geometry to TBP.[30,31]

To confirm the coordination structure of the azido copper complexes in the solution that has been estimated from UV−vis spectral data, the ESR spectroscopic measurements were performed for them. ESR spectra and parameters of **1a**, **2a**, **3a**, and **4a** are presented in Figure 2 and Table 2, respectively. The data of **2a**, **3a**, and **4a** revealing $g_\perp > g_{||} > 2.00$ and $|A_{//}| = 70-82$ G are typical of a five-coordinate trigonal bipyramidal structure around a Cu(II) ion with a d_z2 ground state.[30−32] On the other hand, **1a** showed features with $g_{||} > g_\perp > 2.00$ and $|A_{//}| = 153$ G, which is characteristic for a five-coordinate SP.[33] Thus, the ESR spectra confirm the conclusion drawn from the UV−vis data. As is clear from the spectral patterns in Figure 2, the increase in number of NH_2 groups generated a gradual distortion from idealized trigonal bipyramidal structure, and the $g_\perp$ values increased constantly upon going from **4a** to **2a**. This strongly indicates that the electron donating ability from pyridine nitrogens in

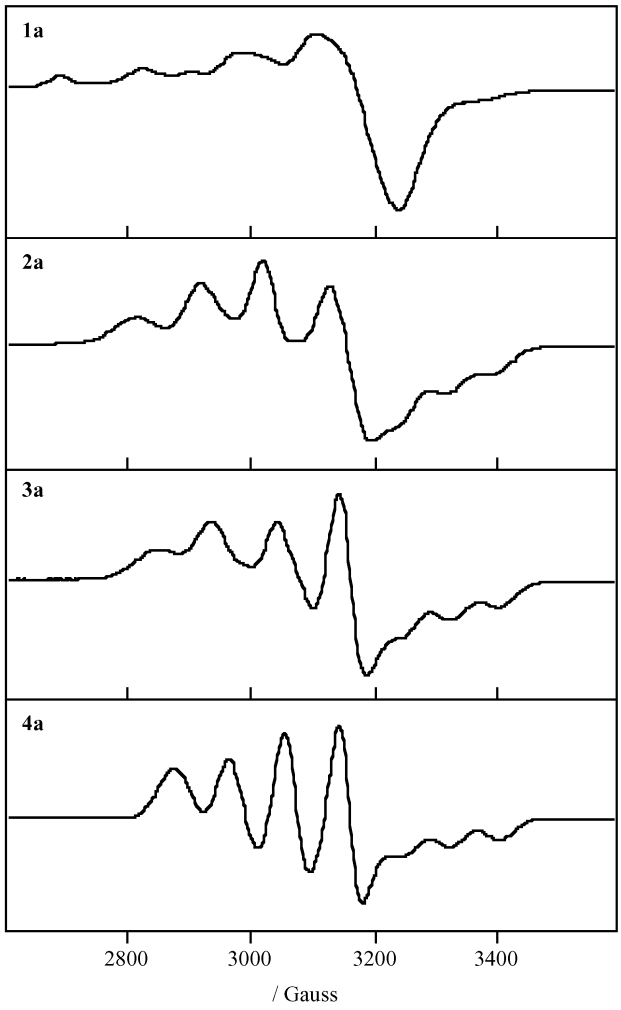

Figure 2. ESR spectra of $[Cu(tapa)(N_3)]^+$ (**1a**), $[Cu(bapa)(N_3)]^+$ (**2a**), $[Cu(mapa)(N_3)]^+$ (**3a**), and $[Cu(tpa)(N_3)]^+$ (**4a**) in MeOH (frequency 9.252 GHz, power 1 mW, modulation amplitude 6.3 G, temperature 77 K.)

the equatorial positions has been weakened to decrease the ligand field splitting. Therefore, the steric repulsion between NH_2 substituent groups and azide ion should elongate the bond lengths between the pyridine nitrogens and Cu(II) ion to weaken the coordination bonding strengths. Taking all the spectroscopic data into consideration, allows suggesting that change in the coordination environment from TBP to SP geometry would depend on the number of NH_2 groups substituted to the ligands. Thus, the steric interaction between NH_2 groups and azide ion should affect geometric structure of the copper complexes. This is similar to steric effect of methyl substituents in the structures of $[Cu(6\text{-}Me_n tpa)(Cl)]^+$ [34] and $[Fe(6\text{-}Metpa)(acac)]^{2+}$ [35] studied previously.

(30) Wei, N.; Murthy, N. N.; Karlin, K. D. *Inorg. Chem.* **1994**, *33*, 6093 and references therein.
(31) Malachowski, M. R.; Huynh, H. B.; Tomlinson, L. J.; Kelly, R. S.; Furbee jun, J. W. *J. Chem. Soc., Dalton. Trans.* **1995**, 31.
(32) Solomon, E. I.; Hanson, M. A. In *Inorganic Electronic Structure and Spectroscopy*; Solomon, E. I., Lever, A. B. P., Eds.; John Wiley & Sons: New York, 1999; pp 1−130.
(33) In the spectrum of **1a** (Figure 2 top), the minor features were also observed at ca. 2940, 3020, and 3390 G, showing the presence of another mononuclear Cu(II) species with a TBP geometry.

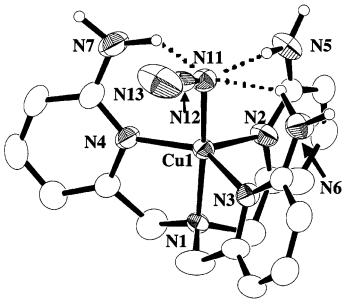

Figure 3. ORTEP drawing of $[Cu(tapa)(N_3)]^+$ (**1a**) with the atomic labeling scheme. Hydrogen atoms are omitted for clarity except for NH protons.

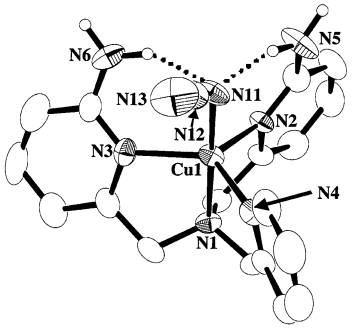

Figure 4. ORTEP drawing of $[Cu(bapa)(N_3)]^+$ (**2a**) with the atomic labeling scheme. Hydrogen atoms are omitted for clarity except for NH protons.

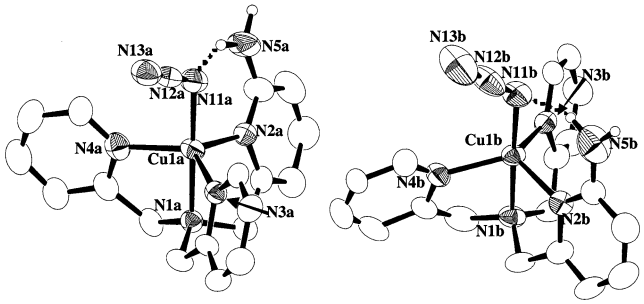

Figure 5. ORTEP drawings of two independent structures of $[Cu(mapa)(N_3)]^+$ (**3a**) with the atomic labeling scheme. Hydrogen atoms are omitted for clarity except for NH protons.

X-ray Crystal Structures of 1a, 2a, 3a, and 4a. We succeeded in the X-ray measurements for all the azido copper(II) complexes $[Cu(L)(N_3)]^+$. The ORTEP diagrams of the cation parts of **1a**, **2a**, **3a**, and **4a** are represented in Figures 3, 4, 5, and 6, respectively. Selected bond lengths and angles for them are summarized in Table 3. The complexes **2a**, **3a**, and **4a** revealed an axially compressed trigonal bipyramidal geometry around the Cu(II) site with the tertiary amine nitrogen of the ligand in one of the axial positions (Cu−N(amine) bond lengths: **2a**, 2.009(8) Å; **3a**, 2.018(7), 2.043(8) Å; **4a**, 2.025(8) Å) and three pyridine nitrogens in the trigonal plane (average Cu−N(pyridine) bond lengths: **2a**, 2.09 Å; **3a**, 2.08 Å; **4a**, 2.08 Å). Another axial position was occupied by an azide anion in the end-on fashion (Cu−N(azide): **2a**, 1.954(9) Å; **3a**, 1.952(9), 1.943(8) Å; **4a**, 1.935(9) Å). Furthermore, the structural environments around the copper sites were evaluated by use of coordination geometric parameter τ ($= (\beta - \alpha)/60$), where α and β represent two basal angles ($\beta \geq \alpha$), introduced by Addison et al.;[36] $\tau = 1$ for an idealized trigonal bipyramidal structure and $\tau = 0$ for perfect square pyramidal geometry. As listed in Table 3, the τ values of **2a**, **3a**, and **4a** are 0.79, 0.87(av), and 0.92, respectively, indicating that ligands bapa, mapa, and tpa form a trigonal bipyramidal structure around Cu(II) center with azide. Since the τ values of **2a** and **3a** are smaller than those of copper complex without NH_2 group, **4a** ($\tau =$ 0.92) and $[Cu(tpa)Cl]^+$ ($\tau = 1.0$)[37] whose structures exhibit almost theoretical TBP geometry, it is clear that the presence of NH_2 amine groups gives rise to some structural distortions for TBP structure. The molecular structure of **1a** (Figure 3) expressed five-coordinate geometry around a Cu(II) center coordinated by the tertiary amine nitrogen of tapa (Cu−N(amine) bond length 2.018(6) Å), three pyridine nitrogens (Cu−N(py) bond length 2.194(7), 2.070(8), and 2.065(7) Å), and azide nitrogen (Cu−N(azide) bond length 1.962(7) Å). The τ value estimated for **1a** ($\tau = 0.48$) demonstrates that the coordination structure is an intermediate between TBP and SP geometries. According to the above structural results and geometric parameter τ, the magnitude of geometrical change from TBP to SP structures becomes large with an increase in the number of NH_2 groups (**4a** < **3a** < **2a** < **1a**). Additionally, these findings permit defining that the steric effect of ligands to copper center is a little smaller than those found in $[Cu(TMQA)(Cl)]^+$ [30] and $[Cu(6\text{-}Me_n tpa)(Cl)]^+$,[34] with SP geometry.

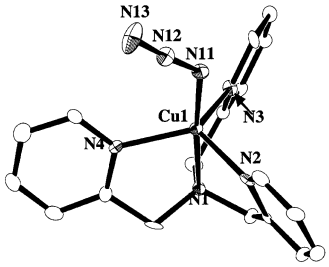

Figure 6. ORTEP drawing of $[Cu(tpa)(N_3)]^+$ (**4a**) with the atomic labeling scheme. Hydrogen atoms are omitted for clarity.

The comparison of bond lengths of the series $[Cu(L)(N_3)]^+$ gave interest findings for functions of NH_2 substitutions. The distance between the copper ion and azide nitrogen becomes longer with increase in the number of NH_2 groups of ligands, **4a** < **3a** < **2a** < **1a**, although the Cu−N bond in equatorial plane of the Cu(II) complex with SP geometry is generally shorter than those in the trigonal plane of the Cu(II) complex with TBP. This indicates that the Cu−N(azide) bond is elongated through the steric interaction between NH_2 groups and the external azide anion. Also, the average distances of the Cu−N(pyridine) bonds tend to increase in the order **4a** (2.08 Å) ≈ **3a** (2.08 Å) < **2a** (2.09 Å) < **1a** (2.11 Å), although the bond lengths between the Cu(II) center and

(34) Nagao, H.; Komeda, N.; Mukaida, M.; Suzuki, M.; Tanaka, K. *Inorg. Chem.* **1996**, *35*, 6809.
(35) Zang, Y.; Kim, J.; Dong, Y.; Wilkinson, E. C.; Appelman, E. H.; Que, L. Jr. *J. Am. Chem. Soc.* **1997**, *119*, 4197.
(36) Addison, A. W.; Rao, T. N.; Reedijk, J.; van Rijn, J.; Verschoor, G. C. *J. Chem. Soc., Dalton. Trans.* **1984**, 1349.
(37) Karlin, K. D.; Hayes, J. C.; Juen, S.; Hutchinson, J. P.; Zubieta, J. *Inorg. Chem.* **1982**, *21*, 4106.

Table 3. Selected Bond Lengths and Angles and τ Values of **1a**, **2a**, **3a**, and **4a**

	1a	**2a**	**3a**		**4a**
		Bond Lengths (Å)			
Cu(1)−N(1)	2.018(6)	2.009(8)	2.018(7)	2.043(8)	2.025(8)
Cu(1)−N(2)	2.194(7)	2.138(9)	2.115(8)	2.102(8)	2.091(10)
Cu(1)−N(3)	2.070(8)	2.097(9)	2.068(9)	2.068(8)	2.066(9)
Cu(1)−N(4)	2.065(7)	2.029(9)	2.033(7)	2.068(9)	2.068(8)
Cu(1)−N(11)	1.962(7)	1.954(9)	1.952(9)	1.943(8)	1.935(9)
N(5)···N(11)	3.05(1)	2.95(1)	2.95(1)	2.84(2)	
N(6)···N(11)	2.87(1)	2.94(2)			
N(7)···N(11)	2.89(1)				
		Bond Angles (deg)			
N(1)−Cu(1)-N(2)	81.7(3)	80.2(4)	80.5(3)	80.8(3)	81.2(3)
N(1)−Cu(1)-N(3)	82.8(3)	80.1(4)	82.2(3)	81.4(3)	80.5(3)
N(1)−Cu(1)-N(4)	81.2(3)	83.3(4)	81.9(3)	80.5(4)	81.0(3)
N(1)−Cu(1)-N(11)	174.0(3)	177.9(4)	178.2(3)	175.9(4)	175.1(4)
N(2)−Cu(1)-N(3)	106.6(3)	107.5(3)	106.7(3)	115.1(3)	114.8(3)
N(2)−Cu(1)-N(4)	101.4(3)	114.7(4)	120.6(3)	113.3(3)	119.9(3)
N(2)−Cu(1)-N(11)	104.1(3)	101.8(4)	100.6(4)	100.8(4)	95.7(4)
N(3)−Cu(1)-N(4)	145.3(3)	130.8(4)	126.3(3)	124.2(3)	117.9(3)
N(3)−Cu(1)-N(11)	96.4(3)	99.6(4)	98.8(4)	94.5(3)	97.4(4)
N(4)−Cu(1)-N(11)	96.3(3)	95.4(4)	96.3(3)	102.3(4)	103.9(4)
		τ values			
	0.48	0.79	0.87	0.86	0.92

pyridine nitrogens are almost typical of those found in the previously reported mononuclear Cu(II) complexes with tetradentate tripodal ligands (2.0−2.2 Å).[30,34,37,38] It is clear that these results are the direct evidence for the presence of the steric repulsion between NH_2 substitutions and azide anion. Thus, such steric interaction can be identified as a primary factor providing a distortion from higher symmetric TBP to SP geometry.

In the cases of **1a**, **2a**, and **3a**, it is interesting that all the bond lengths between the azide nitrogen attached to the copper center and NH_2 nitrogens of the ligands (2.84−3.05 Å) (Table 3) fall in the range of typical hydrogen-bonding distances. This indicates that the fixation of azide anion to the Cu(II) atom is assisted by the intramolecular hydrogen bonding interaction between NH_2 groups and azide ion. Presumably, such an interaction in coordination sphere of metal complexes significantly contributes to fixation of small molecules such as O_2, which could stabilize μ-peroxo-copper intermediates in solution, as described below.

Electrochemical Properties. The cyclic voltammogram for complexes $[Cu(L)(N_3)]^+$ was measured in MeOH under Ar atmosphere. The electrochemical parameters are summarized in Table 1. Those of all azide complexes displayed a single quasi-reversible one electron redox wave. The peak separations ΔE of the redox couples were almost constant (0.09 V), suggesting that a drastic structural change around copper ion did not occur through the Cu(I)/Cu(II) redox behavior. The redox potential values $E_{1/2}$ for the Cu(I)/Cu(II) redox couples shifted to higher potential side in the order **4a** < **3a** < **2a** < **1a**. These results suggest that the electron density on the copper centers decreases with increase in the number of NH_2 substitutions. This is well explained in terms of the structural data of the azido copper complexes and the hydrogen bonding effect of NH_2 groups with azide nitrogen. That is, for comparison of the Cu−N(pyridine) and Cu−N(azide) bond lengths for **1a**, **2a**, **3a**, and **4a**, these bond lengths were elongated in the order **4a** ≈ **3a** < **2a** < **1a** by the steric repulsion between azide and NH_2 groups as mentioned above. Their elongation can be considered to lower the electron donating ability of the pyridines to copper ion, and then result in shift of $E_{1/2}$ to higher potential side.[34] It has been reported that the electron donating atoms coordinated to metal ions interact with hydrogen-bonding atoms to decrease their electron density, which makes the redox potentials of metal complexes shift to the positive side.[39] Therefore, the formation of hydrogen bond between NH_2 groups and azide should decrease the electronegativity of N_3^- nitrogen as electron donor and induce the positive shifts of redox potentials of the copper complexes, especially **1a** and **2a**. Thus, it is concluded that the combination of the steric and hydrogen-bonding effects could dominate the electron donation of the ligands for Cu(II) center to determine the redox potentials of $[Cu(L)(N_3)]^+$.

Synthesis of μ-Peroxo Dinuclear Copper(II) Complexes. It has previously been reported by Karlin et al. that the reaction of Cu(I) complex of tpa with dioxygen gives μ-peroxo dinuclear Cu(II) complex, $[\{Cu(tpa)\}_2(O_2)]^{2+}$.[11,12] To study geometric and electronic structures of μ-peroxo dinuclear Cu(II) complexes $[\{(L)Cu\}_2(O_2)]^{2+}$ and to clarify hydrogen bonding and steric effects of ligands on their formation and decomposition, the reactions of synthetic Cu(I) complexes with dioxygen were investigated. The formulation and physicochemical properties of the synthesized peroxo Cu(II) dimers in MeOH solution were identified by UV−vis, ESR, ESI mass, and resonance Raman spectroscopic analysis, as below.

First, the Cu(I) complexes were prepared by the reaction of each tripodal ligand with an equimolar amount of Cu(I) salt in MeOH or EtOH, but they could not be isolated as good crystals of $[Cu(tapa)]^+$ (**1b**), $[Cu(bapa)]^+$ (**2b**), or

(38) Oberhausen, K. J.; O'Brien, R. J.; Richardson, J. F.; Buchanan, R. M. *Inorg. Chim. Acta* **1990**, *173*, 145.

(39) Ueyama, N.; Terakawa, T.; Nakata, M.; Nakamura, A. *J. Am. Chem. Soc.* **1983**, *105*, 7098.

Table 4. Spectral Data for Dinuclear Peroxo Cu(II) Complexes in MeOH

complex	UV−vis spectral data LMCT[a]/nm (ϵ/$M^{-1}cm^{-1}$)	rR spectral data /cm^{-1} $\nu(^{16}O-^{16}O)$	$\nu(^{18}O-^{18}O)$	$\nu(Cu-^{16}O)$	$\nu(Cu-^{18}O)$	dec. rate $k_{dec}/10^4cm^{-1}$
$[\{(tapa)Cu\}_2(O_2)]^{2+}$ (**1c**)	449 (4620), 684 (400)	853, 819	807, 776	n. d.[c]	n. d.[c]	1
$[\{(bapa)Cu\}_2(O_2)]^{2+}$ (**2c**)	474 (6860), 660 (680)	858	812	547	522	100
$[\{(mapa)Cu\}_2(O_2)]^{2+}$ (**3c**)	500 (9680), 595 (1820)	847	800	544	518	390
$[\{(tpa)Cu\}_2(O_2)]^{2+,b}$ (**4c**)	525 (11500), 590 (7600)	832	788	561	535	[d]

[a] LMCT ($O_2^{2-} \rightarrow$ Cu(II)). [b] Recorded in EtCN solution; refs 12 and 41. [c] Not detected. [d] Not measured.

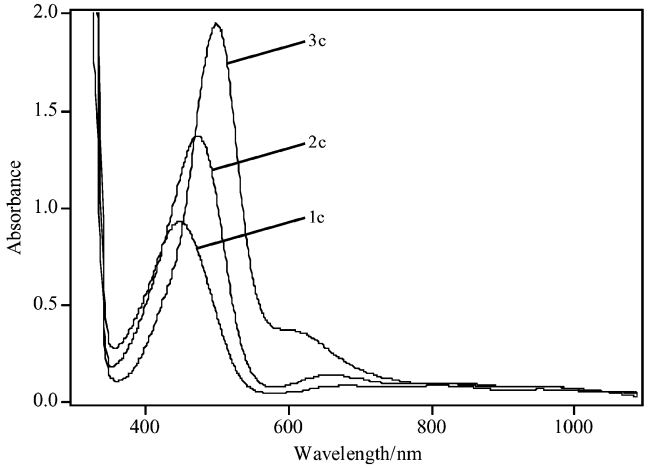

Figure 7. UV-vis spectra of dinuclear peroxo copper(II) complexes (**1c**, **2c**, and **3c**) in MeOH at −75 °C.

$[Cu(mapa)]^+$ (**3b**) suitable for X-ray diffraction analysis because the synthesis condition easily undergoes disproportionation to a Cu(II) salt and copper metal. The use of alcohols is required in preparation of the series $[Cu(L)]^+$, since the ligands having 6-aminopyridine units with a higher polarity can be dissolved only in such solvents. Therefore, in studies on the reactivity of $[Cu(L)]^+$ for dioxygen, the Cu(I) complexes obtained by mixing an equimolar amount of the appropriate ligand and $[Cu(MeCN)_4]X$ (X = PF_6 or ClO_4) were used, and their oxygenation by dioxygen permitted a full generation of the corresponding peroxo Cu(II) complexes. The further spectroscopic characterization and stability of the μ-peroxo dinuclear copper(II) complexes will be described below.

UV−vis, ESR, and ESI Mass Spectroscopies of 1c, 2c, and 3c. Bubbling of dioxygen into MeOH solutions containing the Cu(I) complexes with NH_2-substituted ligands at −75 °C showed a drastic color change from pale yellow to reddish purple or dark brown. Such color changes are allowed to predict the generation of peroxo dicopper adducts, whose spectra and data are shown in Figure 7 and Table 4. The UV−vis spectra of the reaction solutions of **1c**, **2c**, and **3c** exhibited two characteristic peaks in the range 400−650 nm which are assignable to LMCT bands from peroxide to Cu(II) ion. According to the previous papers,[22,40] these bands are assigned to $\pi_\sigma^* \rightarrow d_\sigma$ CT and $\pi_v^* \rightarrow d_\sigma$ CT ones for the shorter and longer wavelength ones, respectively. The shorter wavelength ones shifted toward shorter side with increase in the number of NH_2 groups and simultaneously accompanied by decrease in the peak intensity; λ_{max}/nm (ϵ $M^{-1}cm^{-1}$) = 449 (4620), 474 (6860), and 500 (9680) for **1c**, **2c**, and **3c**, respectively. On the other hand, the longer ones showed the shift to quite opposite side with decrease in peak intensity; λ_{max}/nm (ϵ $M^{-1}cm^{-1}$) = 684 (400), 660 (680), and 595 (1820), for **1c**, **2c**, and **3c**, respectively. The former spectral behaviors are very similar to those of the azide−Cu(II) complexes described above. The d−d transition bands were observed in the wavelength region of 600−835 nm, whose spectral patterns are very similar to each other, although it is difficult to estimate only the d−d bands because of the overlapping of the $\pi_v^* \rightarrow d_\sigma$ CT band. These UV−vis spectra are very similar to that of trans-μ-1,2 peroxo dinuclear Cu(II) complex $[\{(tpa)Cu\}_2(O_2)]^{2+}$ (**4c**) reported previously,[11,12] and, especially, to that of **3c**.[22] The decrease in the intensity of $\pi_v^* \rightarrow d_\sigma$ CT band for peroxo-Cu(II) complexes is attributed to the hindered rotation of the peroxo group by the hydrogen bonding interactions between the peroxo oxygen and NH_2 groups.[22] These facts simply demonstrate that all ligands with NH_2 groups are able to construct the peroxo-Cu(II) complexes.

Upon the use of tpa as ligand in MeOH, the observation of trans-μ-1,2 peroxo dinuclear Cu(II) species was not permitted. Probably, since the peroxide bound to the dicopper center, which is known to have a higher basicity, easily accepts protons from solvent,[41] the peroxo-copper species was destabilized even at low temperature. The result may provide strong evidence that the NH_2 substitutions should sterically protect the peroxide from exogenous environment, which could be one of the factors for stabilization of the peroxo-copper species.

A series of the peroxo complexes **1c**, **2c**, and **3c** was all ESR silent due to the strong antiferromagnetic coupling between the two Cu(II) ions associated with the peroxide bridge.[4] This firmly indicates that the core structures, where dicopper centers are bridged by the peroxide, are rigidly kept in solution. However, after warming the reaction solution under a vigorous flow of Ar, the generation of green copper complexes as ESR active species was observed with disappearance of LMCT bands in UV−vis spectra. This is interpreted as follows: the irreversible oxidation of the copper ions occurs to give mononuclear Cu(II) complexes through a release of the peroxide. Thus, based on the higher basicity of peroxide as mentioned above, it is very difficult to perform reversible dioxygen binding function by synthetic copper complexes in the protic solvent MeOH.

The formation of μ-peroxo dicopper(II) species was confirmed from ESI mass spectral measurements of a MeOH

(40) Pate, J. E.; Cruse, R. W.; Karlin, K. D.; Solomon, E. I. *J. Am. Chem. Soc.* **1987**, *109*, 2624.

(41) Paul, P. P.; Tyeklár, Z.; Jacobson, R. R.; Karlin, K. D. *J. Am. Chem. Soc.* **1991**, *113*, 5322 and references therein.

solution containing **1b** treated with $^{16}O_2$ (Figure S1 in the Supporting Information). The spectrum afforded positive ion peak clusters at *m*/*z* 414, whose observed mass and isotope pattern corresponded to the $[\{(tapa)Cu\}_2(^{16}O_2)]^{2+}$ ion. In the use of $^{18}O_2$ instead of $^{16}O_2$, the feature at *m*/*z* 414 shifted to 416, which is consistent with the increased mass of $^{18}O_2$ relative to $^{16}O_2$ (Figure S1). These data provide evidence for the generation of a μ-peroxo dinuclear Cu(II) complex formulated as $[\{(tapa)Cu\}_2(O_2)]^{2+}$ in solution. Interestingly, the intense brown color of **1c** was maintained throughout the course of the mass spectroscopic experiments. This strongly suggests that the peroxo Cu(II) dimer with tapa is very stable even in protic solvent. Thus, the hydrogen bonds between NH_2 hydrogens of ligand and peroxy oxygens could realize the high stability of μ-peroxo dinuclear Cu(II) complex.

On the reaction of the Cu(I) complex **2b** with $^{16}O_2$ and/or $^{18}O_2$, the ESI mass spectra afforded positive ion peak clusters at *m*/*z* 399 and 401, respectively. These mass data and isotope patterns show that **2c** can be best formulated as $[\{(bapa)Cu\}_2(O_2)]^{2+}$. Notably, the intensity of these peaks was much weaker than that observed in **1c**. On the other hand, the species **3c** and **4c** never give the positive mass peaks derived from the expected peroxo complexes $[\{(L)Cu\}_2(O_2)]^{2+}$. Thus, it is clear from the detection of **1c** and **2c** by ESI mass spectroscopy that the successful stabilization of the peroxo dinuclear copper(II) complexes should be achieved by the use of the artificial hydrogen-bonding interaction.

Resonance Raman Spectroscopy of 1c, 2c, and 3c. Resonance Raman spectra of **1c**, **2c**, and **3c** in MeOH were studied at −75 °C by using 476.5 nm laser excitation (Figure S2). The resonance Raman spectral data are listed in Table 4. In the reactions of **1b**, **2b**, and **3b** with $^{16}O_2$, the resonance-enhanced Raman features were observed at 853, 858, and 847 cm^{-1}, respectively. These features shifted to 807, 812, and 800 cm^{-1} when $[Cu(L)]^+$ reacted with $^{18}O_2$ in place of $^{16}O_2$. The degrees of the isotope shift are in agreement with the theoretical value $\Delta\nu(O-O)$ = ca. 49 cm^{-1}, allowing assignment of the features as the intraperoxide stretching vibration. These stretching vibrations were in the range typical for $\nu(O-O)$ of the (hydro)peroxo Cu(II) species [13,41,42] and were found in a higher frequency region as compared with those observed in **4c** ($\nu(^{16}O-^{16}O/^{18}O-^{18}O)$ = 832/788 cm^{-1})[43] and terminal peroxo dinuclear Cu(II) complexes $[Cu_2(XYL-O-)(OO)]^{2+}$ ($\nu(^{16}O-^{16}O)$ = 803 cm^{-1}).[40] The strength of these O−O bonds allows demonstration of the lower electron density on the antibonding π^* orbitals of peroxide.[42,44] This is supported by the observation of weakened intensity of the bands correlated with the charge transfer (CT) transitions from the peroxide π^* orbital to Cu d orbital (vide infra).[45] Interestingly, this observation is similar to those found in the protonation of peroxide as follows.: Raman studies on the peroxo-alkali metals and their protonated peroxide salts showed an increase in $\nu(O-O)$ frequency, from 740−790 cm^{-1} for peroxide to 840−880 cm^{-1} for hydroperoxide.[46] Other examples for the increase upon the protonation of peroxide have been reported: O_2^{2-} (750 cm^{-1}),[46] HOO^- (836 cm^{-1}),[47] H_2O_2 (864−881 cm^{-1}).[48,49] Thus, the intramolecular hydrogen bond between the peroxide and NH_2 substituents could give a similar effect for electronic structure of peroxo-copper unit induced by the formation of a peroxide−hydrogen (OO−H) covalent bond.[42]

The resonance Raman spectra of **1c** also showed a minor band at 819 cm^{-1}, which shifted to 776 cm^{-1} in the reaction with $^{18}O_2$ ($\Delta\nu(O-O)$ = 43 cm^{-1}). The bands identified as O−O stretching vibration suggest the existence of another peroxo dicopper isomer. The finding could be explained by the substituent effect of tapa ligand that tends to generate at least two Cu(II) complexes (minor and major) with different coordination geometries in solution. To confirm the effect of hydrogen-bonding interaction between NH_2 groups and the peroxide oxygen on the stability, the resonance Raman spectrum of **1c** in CD_3OD was performed (Figure S3). The $\nu(O-O)$ vibration was observed as two bands at 854 and 820 cm^{-1}, both of which slightly shifted toward the higher energy side by 1 cm^{-1}. This indicates that the peroxo complex has been stabilized by intramolecular hydrogen bonds. Furthermore, the higher energy shifts of both bands imply the presence of two kinds of peroxo species.

In the resonance Raman spectroscopic measurements on the reaction of **2b** and **3b** with $^{16}O_2$, Raman bands were also detected at 547 and 544 cm^{-1}. These bands were shifted to 522 and 518 cm^{-1}, respectively, upon the use of $^{18}O_2$. The observation of theoretical isotope shift $\Delta\nu(Cu-O)$ = ca. 25 cm^{-1} permitted identification of these bands as the copper−oxygen stretching vibrations. Unfortunately, we did not succeed in observation of the bands from the Cu−O vibration for the peroxo complex **1c**. The observed Cu−O stretching frequencies in **2c** and **3c** are found at a little lower frequency as compared with that in **4c** ($\nu(Cu-^{16}O)$ = 561 cm^{-1} (Table 4)),[12,41] manifesting the formation of relatively weak Cu−O bonds. Presumably, the observed weak Cu−O bonds are attributed to both the steric and hydrogen-bonding interactions between the bridged peroxide and NH_2 groups. On the basis of the above spectroscopic features, the Cu(I) complexes with NH_2-substituted ligands can react with dioxygen to afford trans-μ-1,2 peroxo dinuclear Cu(II) complexes formulated as $[\{(L)Cu\}_2(O_2)]^{2+}$ (Scheme 1).

To Assess Steric and Hydrogen Bonding Effects of Ligands on the Stability of μ-Peroxo Dinuclear Copper(II) Complexes. It has been reported that the Cu(I) complexes with tripodal pyridylamine ligands, $[Cu(TMQA)]^+$ [50] and

(42) Root, D. E.; Mahroof-Tahir, M.; Karlin, K. D.; Solomon, E. I. *Inorg. Chem.* **1998**, *37*, 4838 and references therein.
(43) Baldwin, M. J.; Ross, P. K.; Pate, J. E.; Tyeklár, Z.; Karlin, K. D.; Solomon, E. I. *J. Am. Chem. Soc.* **1991**, *113*, 8671.
(44) Chen, P.; Fujisawa, K.; Solomon, E. I. *J. Am. Chem. Soc.* **2000**, *122*, 10177.
(45) Baldwin, M. J.; Root, D. E.; Pate, J. E.; Fujisawa, K.; Kitajima, N.; Solomon, E. I. *J. Am. Chem. Soc.* **1992**, *114*, 10421.
(46) Eysel, H. H.; Thym, S. Z. *Anorg. Allg. Chem.* **1975**, *411*, 97.
(47) Vasquez, G. J.; Buenker, R. J.; Peyerimhoff, S. D. *Chem. Phys.* **1989**, *129*, 405.
(48) Giguére, P. A.; Shrinivasan, T. K. *J. Raman Spectrosc.* **1974**, *2*, 125.
(49) Huang, H. H.; Xie, Y.; Schaefer, H. F. *J. Phys. Chem.* **1996**, *100*, 6076.
(50) Karlin, K. D.; Wei, N.; Jung, B.; Kaderli, S.; Niklaus, P.; Zuberbühler, A. D. *J. Am. Chem. Soc.* **1993**, *115*, 9506.

Scheme 1. Proposed Coordination Structure of the trans-μ-1,2 Peroxo Dinuclear Copper(II) Complex with Tripodal Tetradentate Ligand Having Amino-Substituent Groups

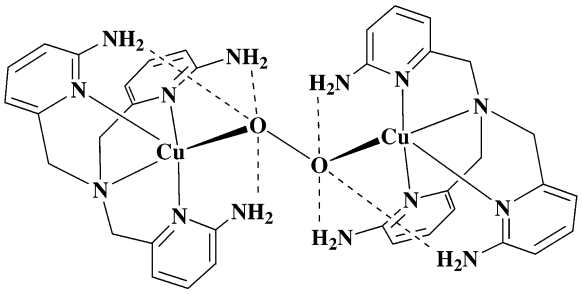

$[\{Cu(tapa)\}_2O_2]^{2+}$

$[Cu(6\text{-}Me_3tpa)]^+$, [51] could not react with dioxygen. This is because the steric hindrance around copper ion constructed by methyl substituent groups at 6-position of pyridine or quinolyl groups protected the approach of dioxygen to copper center. However, we observed that even **1b** having NH_2 groups introduced at 6-positions of all three pyridines could easily react with dioxygen to afford trans-μ-1,2 peroxo Cu(II) dimer. The differences indicate that the steric effect of amino groups is weaker than those found in methyl and 2-quinolyl groups. This feature is also supported from structural results of $[Cu(L)(N_3)]^{2+}$. Furthermore, it is worthy to note that the number of NH_2 substituent groups governs the stability of $[\{(L)Cu\}_2(O_2)]^{2+}$. Thus, these findings allow deduction that hydrogen-bonding interaction achieved by NH_2 groups is a primary factor for the stabilization of peroxo-copper species.

To assess such specific effects of NH_2-introduced ligands on the generation of stable peroxo dicopper species, the comparison of formation and decay rates of the series $[\{(L)Cu\}_2(O_2)]^{2+}$ were carried out. The formation of the peroxo complexes **1c**, **2c**, and **3c** at -75 °C was followed by monitoring increase of the bands at 449, 474, and 500 nm, respectively. In result, the reactivity of the Cu(I) complexes for dioxygen becomes slow with increase in the number of NH_2 groups. The results appear to be reasonable because the ligands making Cu(I)/Cu(II) redox couple more positive are known to give a thermodynamically stable Cu(I) complex to prevent the oxidation by dioxygen. Indeed, the order of low reactivity of $[Cu(L)]^+$ for dioxygen is consistent with that found in the positive shift of redox potential. On the other hand, the comparison of decay rate k_{dec} of $[\{(L)Cu\}_2(O_2)]^{2+}$, as summarized in Table 4, showed that the peroxo-copper complexes become stable upon going from **3c** to **1c**. It is obviously suggested that the thermal stability of $[\{(L)Cu\}_2(O_2)]^{2+}$ is governed by the number of NH_2 substituent groups. Therefore, we speculate that the hydrogen-bonding interaction between amine hydrogens and peroxy oxygens, which is similar to those observed in $[Cu(L)(N_3)]^+$, should contribute to stable coordination of the peroxide. In fact, we have first succeeded in preparation and isolation of hydroperoxo Cu(II) complex, $[Cu(bppa)(OOH)]^+$, using the BPPA ligand having two hydrogen-bonding pivalamido groups (BPPA = bis(6-pivalamido-2-pyridylmethyl)(2-pyridylmethyl)amine).[52]

The effect of hydrogen bonding interaction, as was expected, was detected also in the results of Raman spectral data (Table 4); the O−O stretching vibrations increased in the order **4c** < **3c** < **2c**, which represents an increase in the O−O bond strengths of the peroxide bound to dicopper center. However, the O−O bond frequency of **1c** was observed in a shorter wavenumber region than the expected one. This may be explained by difference in the coordination geometries of the μ-peroxo dicopper complexes: that is, as described in the section on the crystal structures of the azide complexes, **2a**, **3a**, and **4a** form a trigonal bipyramidal geometry, whereas **1a** gives a square-pyramidal one.

Also, the thermal stability of peroxo-copper complexes was expected to increase with increase in the strength of O−O bonds if these decompositions predominantly occurred via O−O bond cleavage, which have been supposed in oxygen-activating enzymes with copper or iron as active site.[2,3,53,54] Indeed, the decomposition rate became faster in the order **1c** < **2c** < **3c**, as shown in Table 4, which corresponds to the number of hydrogen bonds. It is clear that the stability of the peroxo complexes increases with increase in the number of hydrogen bonds and increases with increase in the O−O bond energy, as described in the above Raman spectral section. On the basis of the above results, we can conclude that the μ-peroxo dinuclear copper complexes can be formed even in a sterically restricted environment through the strong fixation by hydrogen-bonding interaction due to NH_2 groups.

Relationship between Coordination Structure and Electronic Property of μ-Peroxo Dinuclear Copper(II) Complexes. In the comparison of UV−vis spectral data (Table 4), the CT bands constantly shifted toward short-wavelength region and the intensities decreased in the order **1c** < **2c** < **3c** < **4c**. Surprisingly, this trend represents the dependence on the number of NH_2 amine groups of ligands and is comparable to that observed in LMCT bands of $[Cu(L)(N_3)]^+$. As a predominant cause for the short-wavelength shift of the CT transitions, the hydrogen-bonding interaction of NH_2 hydrogens with peroxy oxygens is considered. Such intramolecular interaction could decrease the electron density on the peroxide strongly to stabilize the peroxide π^* orbitals in **1c**, **2c**, and **3c** relative to those in **4c**. At a time, this stabilization should increase the energy gaps between the π^* and Cu d orbitals to occur the high-energy π^*-to-d CT transitions. Thus, the increase of hydrogen bonding stabilizing the peroxide-based molecular orbitals permits observation of the short-wavelength shift of the related CT bands.

Summary and Conclusions

The physicochemical properties of the series of mono-/di-nuclear Cu(II) complexes with N_3^- and μ-O_2^{2-} were

(51) Uozumi, K.; Hayashi, Y.; Suzuki, M.; Uehara, A. *Chem. Lett.* **1993**, 963.

(52) Wada, A.; Harata, M.; Hasegawa, K.; Jitsukawa, K.; Masuda, H.; Einaga, H. *Angew. Chem., Int. Ed.* **1998**, *37*, 798.

(53) Que, L., Jr.; Ho, R. Y. N. *Chem. Rev.* **1996**, *96*, 2607.

(54) Sono, M.; Roach, M. P.; Coulter, E. D.; Dawson, J. H. *Chem. Rev.* **1996**, *96*, 2841.

studied; the steric and hydrogen bonding effects of NH_2 groups were examined. The data of the azido copper complexes **1a**, **2a**, **3a**, and **4a** in the solution and solid states revealed that the steric interaction of NH_2 groups with the coordinated azide anion is an important factor to determine the coordination geometry around the copper center. The elongation of $Cu-N_{py}$ bonds derived from the steric repulsion between NH_2 groups and azide ion reduced electron donation of pyridines to lead to the positive shift of redox potentials of the copper complexes. All distances between the azide and NH_2 in the crystal structures are identical to typical hydrogen-bonding distances, which is responsible for the stable coordination of azide.

Fortunately, since the Cu(I) complexes with bapa and mapa ligands were isolated as a precipitate (although that with tapa was not obtained), the reactivity of the Cu(I) complexes with dioxygen and substituent effects of ligands on the stability of the trans-μ-1,2 peroxo Cu(II) dimers generated were able to be investigated using the Cu(I) complexes with tapa, bapa, and mapa. On the basis of the spectroscopic analyses for **1c**, **2c**, and **3c**, both the formation and decay rates become slow with increase in the number of NH_2 substituents. The thermal stability of these peroxo adducts was raised with increase in numbers of the hydrogen-bonding interaction between NH_2 groups and the peroxide. Strikingly, the strength of the hydrogen-bonding interaction, which could decrease the electron density of the peroxide as charge donor, dominates the electronic properties correlated with the π^*-to-d_σ CT transitions and peroxide-based stretching vibrations ν(O−O) and ν(Cu−O). Thus, we deduced that the stability of $[\{(L)Cu\}_2(O_2)]^{2+}$ is determined by the formation of the peroxo-copper units in sterically restricted environment and their strong fixation by hydrogen-bonding interaction.

In the present studies, the elucidation for the ligand effects stabilizing the peroxo-copper species could provide valuable insights in the stabilization mechanisms of copper−oxygen intermediates utilized by copper-containing proteins in biological systems,[1−3] and lead to the development of fundamental understanding of the copper−oxygen interactions.[4−10]

Acknowledgment. This work was supported partly by a Grant-in-Aid for Scientific Research from the Ministry of Education, Science, Sports, and Culture of Japan (H.M.), and supported in part by a grant from the NITECH 21st Century COE Program (S.Y. and H.M.), for which we express our thanks. A.W. is grateful to the Japan Society for the Promotion of Science for the JSPS Research Fellowship for Young Scientists.

Supporting Information Available: Crystallographic files (CIF); and experimental procedures, Figures S1−S3 (PDF). This material is available free of charge via the Internet at http://pubs.acs.org.

IC0496572